Soft Matter

Volume 1 | Number 1 | Jan 2013 | Pages 1–100

Soft Matter

www.rsc.org/softmatter

ROYAL SOCIETY OF CHEMISTRY

ROYAL SOCIETY OF CHEMISTRY

www.rsc.org/softmatter

We actively control interfacial phenomena by optically trapping the interface in phase separated colloid-polymer mixtures using the gradient forces of a strongly focussed laser beam parallel to the interface.

Optical trapping of interfaces at ultra-low interfacial tension[†]

A. A. Verhoeff[*a], **F. A. Lavergne**[a], **D. Bartolo**[b], **D. G. A. L. Aarts**[a] **and R. P. A. Dullens**[a]

We achieve active control of interfacial phenomena by optically trapping the interface using the gradient forces of a strongly focussed laser beam parallel to the interface. We illustrate our technique in a phase separated colloid-polymer mixture by distorting the interface in a very controlled way. The static structure of the manipulated interface as well as its dynamic relaxation behaviour are analysed. Both the statics and dynamics can be related to the capillary wave height-height correlations using the fluctuation dissipation theorem up to surprisingly large deformations of the interface. To underline the novelty and potential of our approach we also show multiple interface distortions and the controlled snap-off of liquid droplets.

With the rapidly growing importance of nanofluidics and the increasing miniaturisation of lab-on-a-chip devices, precise knowledge of the behaviour of interfaces in confinement is urgently needed[1,2]. Importantly, at these length scales molecular fluctuations and interface dynamics strongly influence the transport and the response of the fluids[3–6]. In atomic and molecular systems, the amplitude of interface fluctuations is typically in the (sub)nanometer range, making the relevant interface dynamics experimentally very hard to access. It has been shown that colloidal systems provide a very convenient model system to explore the interface dynamics in great detail[3,7]. As the interfacial tension in colloidal systems is ultra-low, typically of the order of nN/m, the thermal roughness of the interface is in the micrometer range, which has allowed for the direct imaging of thermal capillary waves in phase separated colloid-polymer mixtures using confocal microscopy[3]. Also, other interfacial phenomena like droplet snap-off, coalescence and wetting have been studied directly in similar colloidal model systems[3,8–10]. Near-critical phase separated microemulsions have an ultra-low interfacial tension as well, which was exploited to study the effect of thermal fluctuations on droplet snap-off[11].

Actively controlling these interfacial phenomena, however, has not yet been achieved in colloidal systems. Recently, several non-contact methods were developed to study interface properties by actively deforming systems like polymer and surfactant solutions, and (phase separated) molecular fluids. Examples include interface distortions with an atomic force microscopy probe[12–14], electric field tweezers[15] or a magnetic sphere above a magnetic particle-laden liquid surface[16]. Furthermore, it has been shown by Ashkin and Dziedzic[17] that one can distort liquid interfaces using the radiation pressure of a focussed laser beam *perpendicular* to the interface. This effect has been studied systematically by Delville and co-workers in near-critical microemulsions[18,19]. Additionally, the gradient forces of a focussed laser beam were employed to actively deform droplets in surfactant stabilized oil-in-water emulsions[20–22]. In order to do similar experiments on droplets or interfaces in colloidal systems, one would need to manipulate multiple particles simultaneously. It has recently been shown theoretically that it is indeed possible to manipulate colloid-polymer mixtures with optical potentials, thereby affecting multiple particles simultaneously and causing density fluctuations and laser-induced phase transitions[23–25].

Here, we use optical trapping to actively deform the fluid-fluid interface in a phase separated aqueous colloid-polymer mixture at an ultra-low interfacial tension. In particular, we use the gradient forces of a laser beam *parallel* to the interface to optically deform the interface in a very controlled way. The static structure of the distorted interface and its dynamic relaxation behaviour after switching off the optical trap are monitored using fluorescence microscopy. Using the fluctuation-dissipation theorem (FDT) we relate both the static structure and dynamic relaxation of the deformed interface to the thermal fluctuations of the unperturbed interface, which are directly imaged using confocal microscopy[3]. We find that FDT holds for surprisingly large deformations of the interface. The robust linear response of the interface makes it possible to extend our experiment to simultaneous manipulations at multiple positions. By going beyond this linear response regime, we finally show how the use of gradient forces of a beam parallel to the interface enables us to achieve the controlled pinching of liquid droplets consisting of a few thousands colloidal particles.

† Electronic Supplementary Information (ESI) available: Videos of interface manipulation and droplet snap-off. See DOI: 10.1039/b000000x/
a Department of Chemistry, Physical and Theoretical Chemistry Laboratory, University of Oxford, South Parks Road, Oxford OX1 3QZ, United Kingdom. Tel: +44 (0)1865 275425; E-mail: lia.verhoeff@chem.ox.ac.uk
b Laboratoire de Physique de l'École Normale Supérieure de Lyon, CNRS, Université de Lyon, allée d'Italie, 69007 Lyon, France.
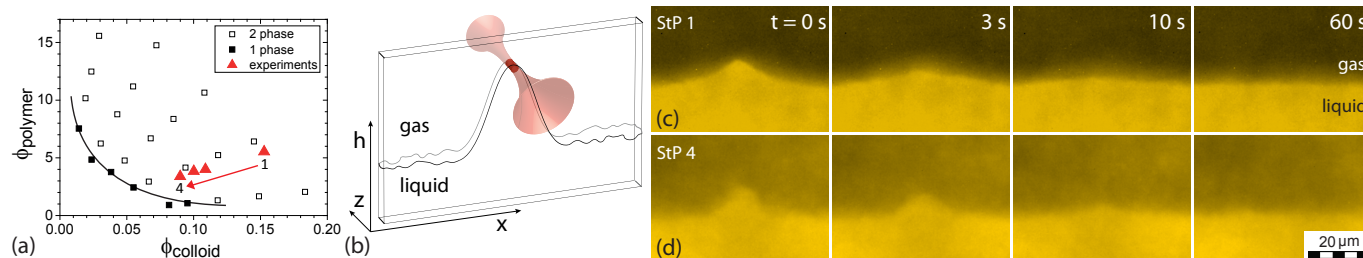
Fig. 1 (a) The experimental phase diagram with the studied state points indicated by red triangles. (b) Schematic drawing of the optical tweezing setup, with the optical trap coming in perpendicular to the imaging plane and parallel to the interface. (c) and (d) show how the colloidal gas-liquid interface is deformed with the optical trap in state point 1 (c) and 4 (d). The laser trap is switched off at $t = 0$ s after which the interface relaxes. The laser power in both cases is 4.5 mW. Video 1 of the ESI[†] shows the interface manipulation and subsequent relaxation of state point 1 at 5× real time and a trapping power of 14.5 mW.

We used aqueous mixtures of poly(methyl methacrylate) (PMMA) particles with a hydrodynamic radius of 123 nm as measured with dynamic light scattering and xanthan polymer ($M_w = 4 \cdot 10^6$ g/mol, $R_g = 264$ nm) in 0.1 M NaCl. The experimental phase diagram is shown in Fig. 1(a). Details on the system preparation can be found in[26]. We studied four different state points, numbered 1 to 4 in the phase diagram in Fig. 1(a), with colloid and polymer volume fraction ϕ_c and ϕ_p, respectively, as indicated in Table 1. State point 1 is far away from and 4 relatively close to the critical point. Capillary waves were recorded in bulk for all state points using confocal laser scanning microscopy (Zeiss, LSM 5 Exciter) on its side, so that the imaging plane was parallel to gravity[3]. From the microscopy images we determined the position of the interface, from which we computed the static and dynamic height-height correlation functions with $g_h(x,t) = \langle h(x,t)|h(x',t')\rangle$. The corresponding expressions for the correlation functions from capillary wave theory for a two-dimensional interface were then fitted to the data[3,26]. The resulting values for the interfacial tension γ, the capillary length L_c, the density difference between gas and liquid phase $\Delta\rho$, and the capillary time τ are given in Table 1.

For the optical tweezing experiments the sample was contained in 15 μm thick cells, unless stated otherwise. These cells were prepared by applying a droplet of a homogenized colloid-polymer mixture onto a microscopy glass slide, adding a trace of 15 μm polystyrene spheres as spacers, covering it with a glass cover slip and sealing it with epoxy glue. Samples were stored upright and trapping experiments were performed after overnight phase separation had finished. The colloidal liquid was trapped with a 1064 nm laser (Coherent) through a 100×/1.4 oil immersion objective (Olympus), with the beam coming in parallel to the gas-liquid interface as shown in Fig. 1(b). The position of the trapping beam was controlled with a spatial light modulator (XY nematic series 512×512, Boulder Nonlinear Systems), which allows for a positioning accuracy of the order of a nanometer[27]. The sample was imaged with a home-built fluorescence microscope, using a 60×/0.7 long working distance objective (Olympus) and a 532 nm laser (CNI laser) for illumination. Imaging was performed with a 4 mega pixel Ximea CCD colour camera. We performed identical optical tweezing experiments with a colloid-polymer mixture in heavy water, which does not absorb the infra-red laser light and consistent results where obtained, showing that heating effects are insignificant.

We deform the colloidal gas-liquid interface by slowly moving the optical trap from the liquid phase into the gas phase. The interface follows the trap and adopts a stationary profile when the trap is stopped at a given height as shown in Fig. 1(c) and (d) at $t = 0$. After switching off the trap the interface relaxes to its original position (Fig. 1(c) and (d) for $t > 0$). See also video 1 of the ESI[†]. Note that the interface is significantly rougher and the contrast poorer in state point 4 (Fig. 1(d)) compared to state point 1 (Fig. 1(c)), which is expected upon approaching the critical point. Upon further approaching the critical point the interface fluctuations become so large and the contrast between the colloidal gas and liquid phases so small that interface manipulation becomes impossible.

In Fig. 2(a) we present the static interface profiles for identical distortions of around 5 μm for the four different state points. We observe that upon approaching the critical point

Table 1 Properties of the state points (StP) as determined from capillary wave analysis. ϕ_c and ϕ_p are the colloid and polymer volume fraction respectively, γ the bulk interfacial tension, L_c the capillary length, $\Delta\rho$ the density difference between gas and liquid phase, and τ the capillary time.

StP	ϕ_c	ϕ_p	γ [nN/m]	L_c [μm]	$\Delta\rho$ [kg/m³]	τ [s]
1	0.15	5.6	68	6.7	163	11.7
2	0.11	4.0	21	5.5	73	12.1
3	0.10	3.8	14	4.9	62	14.1
4	0.09	3.4	9.5	4.8	43	18.0

Fig. 2 (a) Static interface profiles normalised to the maximum height h_0 (~ 5 μm) for the four different state points. Trapping power is 4.5 mW. Solid lines represent fits using Eq. 3. (b) Dynamic interface profiles as a function of time after switching off the optical trap (trapping power 15 mW). The height is normalised to h_0 (~ 12 μm) for all state points. Solid lines represent fits using Eq. 5. (c) Values for the capillary length obtained from the fits (open circles) and from capillary wave analysis (closed squares). (d) Values for the capillary time obtained from profile fits (open circles) and from capillary wave analysis (closed squares). The open triangle denotes the capillary time obtained from a two dimensional interface profile in a 50 μm thick sample cell.

the profile becomes narrower, indicating a smaller capillary length, which is in agreement with the capillary wave experiments (see Table 1). The relaxation of the interface after switching off the trap at $t = 0$ s is shown for all state points in Fig. 2(b). The profiles are normalised with the height at $t = 0$, which is around 12 μm for all state points. Upon approaching the critical point the relaxation becomes slower, corresponding to a larger capillary time, again in qualitative agreement with the capillary wave results (see Table 1). The shoulder that is visible in the dynamic profile of state point 4 is the result of thermal fluctuations, which are quite prominent this close to the critical point.

To quantitatively describe the static and dynamic profiles, we note that in the limit of small deformations, i.e. the linear regime, the time-dependent profile of the manipulated interface $h(x,t)$ can be related to the capillary wave correlation functions $g_h(x,t)$ using the fluctuation dissipation theorem (FDT). In particular, FDT states that the response $R(x,t)$ of the interface to a small force is equal to $R(x,t) = g_h(x,t)/k_BT$. For a point force f located at position $x = 0$ and present from

time $t = -\infty$ to $t = 0$, the interface height $h(x,t)$ is given by

$$h(x,t) = \frac{f}{k_BT} g_h(x,t). \tag{1}$$

The trapped interface in these thin sample cells was found to be invariant along the optical axis, so using the correlation function $g_h(x,t)$ for a line interface, we obtain the shape of the manipulated interface as a function of time:

$$h(x,t) = \frac{fL_c}{\pi\Gamma} \int_0^\infty \frac{e^{i\bar{q}|x|/L_c - \omega_q t}}{\bar{q}^2 + 1} d\bar{q}. \tag{2}$$

Here, f is the force applied at $x = 0$ and $L_c = \sqrt{\gamma/\Delta\rho g}$ with g the gravitational acceleration. Note that Γ in the prefactor is the line tension, defined as $\Gamma = \gamma b$ with b the sample thickness. The dispersion relation ω_q gives the decay rate of each mode with dimensionless wave vector $\bar{q} \equiv qL_c$ and is given by $\omega_q = (\bar{q} + 1/\bar{q})/2\tau$.[3] The capillary time $\tau = L_c\eta/\gamma$, where η is the sum of the viscosities of the colloidal liquid and gas phases.

The static interface profile $h(x)$ is now easily obtained by integrating Eq. 2 at $t = 0$:

$$h(x) = \frac{fL_c}{2\Gamma} e^{-|x|/L_c}. \tag{3}$$

We fit this expression to our experimental static profiles as shown by the solid lines in Fig. 2(a). In general, the agreement is excellent. There is some discrepancy only very close to the trap, which is due to the fact that the assumption that the optical trap acts as a point force breaks down. Especially closer to the critical point, the optical trap violates the point force approximation as it attracts particles from a wider range, and as a consequence the fit somewhat overshoots the experimental data at $x = 0$. From fitting our data with Eq. 3, we obtain values for the capillary length, which are in very good agreement with the ones we find from capillary wave analysis (see Fig. 2(c)).

Now that we have shown that FDT successfully relates the static interface profiles to the capillary wave spectrum, we can use the prefactor $fL_c/2\Gamma$ in Eq. 3 to calculate the force that the optical trap exerts on the interface. If we do so for the fits in Fig. 2 for state point 1 and 4, using the value for the interfacial tension obtained from the capillary wave analysis, we find a force of 1.8 ± 0.3 and 0.5 ± 0.1 pN respectively. For comparison, we consider the work to lift the interface, which is given by the sum of the change in gravitational and interfacial energy: $W = \Delta E_\gamma + \Delta E_g$. The work W equals the product of the force f and the height $h_{\max}$ over which the interface is lifted, so that

$$fh_{\max} = \Gamma\Delta L + \frac{b}{2}\Delta\rho g \int_{-L_0/2}^{L_0/2} h(x)^2 dx, \tag{4}$$

where $\Delta L = L - L_0$ is the increase in interface length. If we calculate this force from the experimental profiles of state point 1 and 4, we find a force of 1.7 ± 0.5 and 0.24 ± 0.07 pN respectively, which is in good agreement with the values obtained from the prefactor. Note that the force calculated from the prefactor in Eq. 3 is a slight overestimation as the fit overshoots the experimental profile somewhat at $x = 0$, especially for state point 4 as explained above.

Analogously to the static profile, we obtain an expression for the relaxation of the interface after the trap has been switched off by setting $x = 0$ in Eq. 2, so that

$$h(t) = \frac{fL_c}{\pi\Gamma} \int_0^\infty \frac{e^{-\omega_{\bar{q}}t}}{\bar{q}^2 + 1} d\bar{q}. \tag{5}$$

The experimental dynamic profiles are well described by Eq. 5 as is evident from the solid lines in Fig. 2(b). The obtained values for the capillary time are given in Fig. 2(d) alongside the corresponding values from the capillary wave analysis. We find that the values for τ as obtained from the interface relaxation are consistently larger than what we obtain from capillary wave analysis. We attribute this to wall and flow effects in the 15 μm thin sample cell. Due to the confinement, changes in the Laplace pressure, contact line movement as well as the generation of a Poiseuille flow may play a significant role in slowing down the relaxation. Note also that the colloidal liquid completely wets the glass wall[28]. To test this we trapped the colloidal gas-liquid interface of state point 2 in a 50 μm thick sample, which is much larger than the capillary length. To fit our data, we now use the $g_h(x,t)$ for a radially symmetric 2D interface[3] in Eq. 1, which gives $h(t) = \frac{f}{2\pi\gamma}K_0(t/\tau)$, where K_0 is the modified Bessel function of the second kind. The capillary time we obtained in this case is in very good agreement with the one from capillary wave analysis (see open triangle in Fig. 2(d)), which indeed confirms that confinement effects are leading to a slower relaxation.

We now take advantage of the linear response of the interface over a wide range of pulling forces to extend our experiments to more complicated interface distortions, an example of which is demonstrated in Fig. 3(a-c) and video 2[†]. The figure shows an interface at state point 1 deformed by two optical traps simultaneously. These profiles can be very well described by a simple superposition of static profiles (Eq. 3), using the capillary length found from capillary wave analysis. The fact that multiple distortions are additive is another confirmation that despite the rather large deformations of the interface, we are still in the linear regime where FDT applies. In fact, we find that we remain in the linear regime up to the point where the deformation becomes unstable and a droplet snaps off. This directly leads to another experiment that is uniquely possible in our setup, which is the optically controlled pinch-off of liquid droplets from the bulk liquid phase. An example thereof is shown in Fig. 3(d-g) and video 3[†] for state point 1,
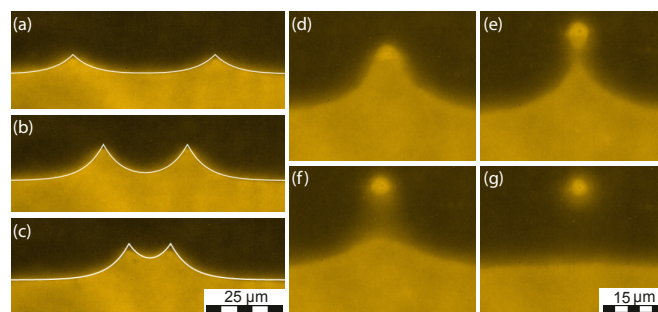
Fig. 3 (a-c) The colloidal gas-liquid interface at state point 1 manipulated by two laser traps simultaneously. The laser power is 18.5 mW for each trap. A superposition of static profiles (Eq. 3) using the capillary length from the capillary wave analysis (white line) describes the profiles very well. (d-g) A droplet of colloidal liquid is pinched-off from the bulk liquid at state point 1 using optical trapping. The laser power is 24 mW. See also video 2 and 3 in the ESI[†], which shows both experiments at 5× real time.

where we lift the interface so high that a droplet is snapped off. As we are trapping parallel to the interface, the droplets are formed in a very reproducible manner and remain stable until the optical trap is switched off.

In conclusion, we have achieved active control of interfacial phenomena in colloid-polymer mixtures with an ultra-low interfacial tension using optical trapping *parallel* to the interface. This experimental framework makes it now possible to address a wide variety of interfacial phenomena in great detail, with particular relevance to strongly confined interfaces.

Acknowledgements

References

1 L. Bocquet and E. Charlaix, *Chem Soc Rev*, 2010, **39**, 1073–95.
2 L. Bocquet and P. Tabeling, *Lab Chip*, 2014, **14**, 3143.
3 D. G. A. L. Aarts, M. Schmidt and H. N. W. Lekkerkerker, *Science*, 2004, **304**, 847.
4 M. Majumder, N. Chopra, R. Andrews and B. J. Hinds, *Nature*, 2005, **438**, 44.

5 S. A. Setu, I. Zacharoudiou, G. J. Davies, D. Bartolo, S. Moulinet, A. A. Louis, J. M. Yeomans and D. G. A. L. Aarts, *Soft Matter*, 2013, **9**, 10599.

6 T. Bickel, *Eur. Phys. Lett.*, 2014, **106**, 16004.

7 D. Derks, D. G. A. L. Aarts, D. Bonn, H. N. W. Lekkerkerker and A. Imhof, *Phys. Rev. Lett.*, 2006, **97**, 038301.

8 A. A. Verhoeff and H. N. W. Lekkerkerker, *New. J. Phys.*, 2012, **14**, 023010.

9 Y. Hennequin, D. G. A. L. Aarts, J. H. van der Wiel, G. Wegdam, J. Eggers, H. N. W. Lekkerkerker and D. Bonn, *Phys. Rev. Lett.*, 2006, **97**, 244502.

10 D. G. A. L. Aarts and H. N. W. Lekkerkerker, *J. Fluid Mech.*, 2008, **606**, 275–294.

11 J. Petit, R. D., H. Kellay and J.-P. Delville, *PNAS*, 2012, **109**, 18327.

12 Y. Z. Wang, D. Wu and J. X. Xhang, *Langmuir*, 2007, **23**, 12119.

13 R. Ledesma-Alonso, D. Legendre and P. Tordjeman, *Phys. Rev. Lett.*, 2012, **108**, 106104.

14 D. B. Quinn, J. Feng and H. A. Stone, *Langmuir*, 2013, **29**, 1427.

15 Y. Shimokawa and K. Sakai, *Phys. Rev. E*, 2013, **87**, 063009.

16 S. S. H. Tsai, I. M. Griffiths, Z. Li, P. Kim and H. A. Stone, *Soft Matter*, 2013, **9**, 8600.

17 A. Ashkin and J. M. Dziedzic, *Phys. Rev. Lett.*, 1973, **30**, 139.

18 R. Wunenburger, A. Casner and J.-P. Delville, *Phys. Rev. E*, 2006, **73**, 036314.

19 R. Wunenburger, A. Casner and J.-P. Delville, *Phys. Rev. E*, 2006, **73**, 036315.

20 A. D. Ward, M. G. Berry, C. D. Mellor and C. D. Bain, *Chem. Commun.*, 2006, **2006**, 4515.

21 D. A. Woods, C. D. Mellor, J. M. Taylor, C. D. Bain and A. D. Ward, *Soft Matter*, 2011, **7**, 2517.

22 D. Tapp, J. M. Taylor, A. S. Lubansky, C. D. Bain and B. Chakrabarti, *Opt. Expr.*, 2014, **22**, 4523.

23 I. O. Götze, J. M. Brader, M. Schmidt and H. Löwen, *Mol. Phys.*, 2003, **101**, 1651–1658.

24 R. L. C. Vink, T. Neuhaus and H. Löwen, *J. Chem. Phys.*, 2011, **134**, 204907.

25 R. L. C. Vink and A. J. Archer, *Phys. Rev. E*, 2012, **85**, 031505.

26 E. A. G. Jamie, G. J. Davies, M. D. Howe, R. P. A. Dullens and D. G. A. L. Aarts, *J. Phys.: Condens. Matter*, 2008, **20**, 494231.

27 C. H. J. Schmitz, J. P. Spatz and J. E. Curtis, *Opt. Expr.*, 2005, **13**, 8678.

28 E. A. G. Jamie, R. P. A. Dullens and D. G. A. L. Aarts, *J. Phys. Chem. B*, 2011, **115**, 13168.